Nuclear Inst. and Methods in Physics Research, A 1047 (2023) 167777

Contents lists available at ScienceDirect

Nuclear Inst. and Methods in Physics Research, A

journal homepage: www.elsevier.com/locate/nima

ATHENA: An active target detector for the measurement of total cross sections

D. Blankstein *, D.W. Bardayan, J.M. Allen, C. Boomershine, L.K. Callahan, S. Carmichael, S.L. Henderson, P.D. O'Malley

Department of Physics, University of Notre Dame, Nieuwland Science Hall, Notre Dame, IN 46556, United States of America

ARTICLE INFO

Keywords:
Active target
Multi-sampling ionization chamber
Nuclear astrophysics

ABSTRACT

Experimentally determined cross sections are a critical input for accurately modeling the nuclear processes that take place in a variety of astrophysical environments. A new detector has been designed and constructed to measure the total cross section of nuclear reactions relevant for astrophysics. The Active Target High Efficiency detector for Nuclear Astrophysics (ATHENA) has been constructed and commissioned by a measurement of the $^{12}C + ^{12}C$ fusion reaction. As an active target detector with a segmented anode, efficient measurements of total cross sections over a wide energy range are possible.

1. Introduction

Nuclear reaction rates, informed by experimentally determined cross sections, are an essential component to models of astrophysical environments. With the advent of radioactive beam facilities, previously unmeasured reactions involving radioactive nuclei are now accessible for study. This allows us to probe astrophysical environments where reactions with radioactive isotopes are taking place. Radioactive beams, however, provide a unique set of challenges when compared to measurements with stable beams. Radioactive beams are difficult to produce and are often low in intensity and contain impurities. Therefore, new detectors and techniques are needed to address the challenges that radioactive beams provide.

A traditional method for measuring cross sections involves bombarding a target containing a heavy nucleus with high intensities of light particles such as protons or alpha particles. Arrays of detectors at various angles measure the energy and angular distributions of light ejectiles. Total cross sections are then extracted from the angular measurements; however careful consideration is needed to normalize the measurements. Precise determination of the incident beam, target contaminants, and detector efficiencies are needed. This process is then repeated for multiple energies in order to build a complete picture of the cross section in the astrophysical energy range.

These types of measurements are rarely possible when the beam of interest is radioactive. Depending on the method of production, radioactive beams require careful tuning that is heavily dependent on the incident energy of the stable beam, which can lead to time consuming energy changes. Radioactive beams are often low in intensity making measurements of very low cross sections, as is often the case in nuclear astrophysics, impractical. Finally, radioactive beams are frequently contaminated, making it sometimes necessary to identify incident beam projectiles on an event-by-event basis.

These issues motivated the design and construction of a variety of active target detectors with the goal of studying nuclear reactions on unstable nuclei (see Ref. [1,2] for recent reviews). Active targets can help mitigate the low beam intensities by greatly increasing the target thickness without losing resolution and by having large solid angle coverage and efficiency for detecting the reaction products. The necessity of having the reaction products pass through inert regions of the target before detection is also eliminated. A further advantage is that reaction excitation functions can be measured without changing the beam energy, which can greatly increase the efficiency of the experiment.

One particular type of active target detector that has become popular is the Multi-Sampling Ionization Chamber (MuSIC) [3–5]. While MuSIC detectors were originally developed for use in high-energy heavy-ion experiments [6–8], more recently their use has been extended to low energy nuclear reactions such as the measurement of (α,p) and (α,n) reactions [9]. MuSIC style detectors offer additional advantages such as being able to determine the incident ion on an event by event basis, being able to measure the total cross section populating all final states since the heavy recoil is used to identify when a reaction has occurred, and being relatively simple and cost-effective to construct.

To take advantage of these benefits, the Active Target High Efficiency detector for Nuclear Astrophysics (ATHENA) at the Notre Dame Nuclear Science Laboratory (NSL) has been constructed. ATHENA will

* Corresponding author.
E-mail address: dblankst@nd.edu (D. Blankstein).

https://doi.org/10.1016/j.nima.2022.167777
Received 18 May 2022; Received in revised form 30 October 2022; Accepted 6 November 2022
Available online 15 November 2022

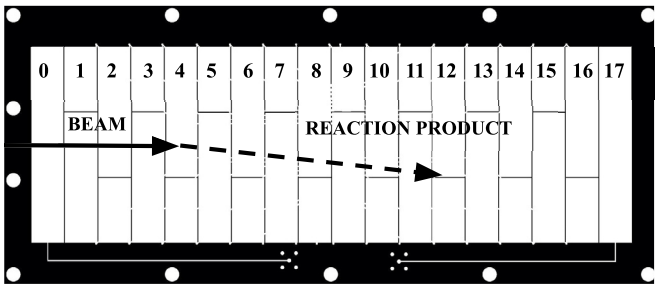

Fig. 1. Schematic of the anode, showing segmented strips. Strips 0 and 17 are used as control strips, where 1–16 are the active strips. Arrows indicate an example of reaction occurring in the 4th active strip, and stopping in the 12th strip.

be used to measure fusion cross sections, as well as perform direct measurements of (α,p) and (α,n) reactions for nuclear astrophysics with radioactive beams produced by the TwinSol facility [10]. This paper will discuss the operating principles of this detector, as well as the technical details of its design. To demonstrate the detector's capabilities, measurements with an alpha source as well as nuclear reaction measurements with accelerated beams will be discussed.

2. Design and operation

2.1. Operating principle

ATHENA is a gas-filled detector designed to measure several points of an excitation function while using a single beam energy. The basic design and operating principle for ATHENA was based upon the Multi-Sampling Ionization Chamber (MUSIC) in operation at Argonne National Laboratory [3] and is similar to MuSIC@Indiana [4] and Encore [5]. ATHENA is an ionization chamber, the basic design of which consists of a gas in a uniform electric field. As charged energetic particles pass through the gas, they lose energy by ionizing the gas particles, forming ion–electron pairs. The ions and electrons are collected by a pair of parallel plates which establish an electric field through which the ions drift. As ion–electron pairs are formed, a voltage signal across the plates will be produced proportional to the number of electrons produced, which in turn gives the energy deposited by the particles. These voltage signals are amplified and processed so that an energy loss spectrum can be obtained.

As an active-target detector, the ionization gas in ATHENA also acts as reaction target for the incoming beam. By performing experiments in inverse kinematics, a heavy beam in the detector can undergo a reaction with the target gas. In choosing a gas that is suitable both as reaction target and ionizing gas, reaction cross sections over a range of energies can be obtained with the use of a segmented anode. Segmenting the detector anode provides measurements of signals that are proportional to the energy loss along a particle track. By measuring this proportional energy loss, the incoming beam can be distinguished from reaction events, as reactions occurring in the detector will produce ions with a different relative energy loss than the beam due to their different atomic numbers. The Bethe formula [11], which describes the energy loss of charged particles in matter, demonstrates that the energy loss of particles is directly proportional to Z^2, where Z is the atomic number of the particle.

Since the beam is continually losing energy as it passes through the detector, reactions in different strips will take place at different center-of-mass energies. The cross sections can therefore be measured over a range of energies without having to change the energy of the beam. The anode is also segmented into beam left/right sections in order to distinguish between reactions and scattering events. In the case of reactions with more symmetric masses, scattering events will have two particles above detection threshold that have similar energy loss curves to the reactions of interest. The left/right segmenting of the anode makes it possible to distinguish these events from reactions because there will be measurable signal in both the left and right strips.

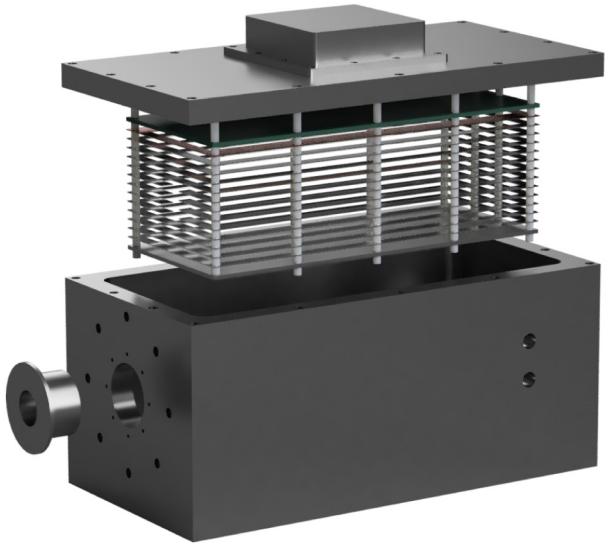

Fig. 2. Rendering of the ATHENA detector. The Anode, Cathode, Frisch-Grid, and field-shaping electrode are all mounted on nylon rods which are affixed to a removable top plate.

There are a number of advantages to using ATHENA for direct measurements of cross sections with radioactive beams. Since the beam and reaction products are measured simultaneously in the same detector, no additional detectors are needed for normalization of the cross section. The energy losses of all beam ions are measured which allows for discrimination of contaminant reactions. The total cross section is measured and no corrections are needed to take into account angular distributions or reactions populating excited states. Finally as mentioned above, ATHENA has the ability to measure the excitation function with a single beam energy, saving time that would otherwise be needed to change beam energies and/or re-tune the beam. The major disadvantages are the beam rate must be limited in order to reduce pile-up and data acquisition dead time.

2.2. Design

The detector consists of a rectangular 38 x 18 x 13 cm aluminum chamber with removable top and bottom plates as well as entrance and exit apertures that allow the beam to pass through. A removable window holder is mounted at the entrance aperture on which 3-6 μm Mylar is epoxied to isolate chamber gas from vacuum. As seen in Fig. 2, the integral components of the ionization chamber are mounted on the removable top plate which also houses feedthroughs for the various signals.

The main components of the detector consist of a cathode, segmented anode, Frisch-grid, and field cage electrodes (see Fig. 3) which are mounted on nylon threaded rods with nylon spacers between them to ensure proper electrical isolation. The anode and cathode establish the electric field, while the field cage electrodes ensure a uniform field throughout the active region. The Frisch-grid is located between the cathode and anode and held at an intermediate voltage in order to shield the anode from drifting positive ions which would otherwise provide a position dependence on the signal pulse height. Biases on the anode typically ranged from (positive) 50–150 V while the cathode was typically biased between (negative) 300–1000 V. Maximum biases were dependent on the type of gas in the chamber, as helium gas has a lower maximum voltage before breakdown occurs.

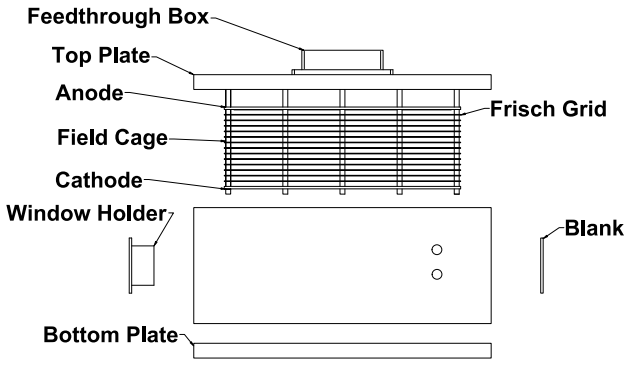

Fig. 3. CAD drawing of ATHENA with the individual components identified.

ATHENA was designed to have a similar split-anode geometry to the MUSIC detector which demonstrated a capability to effectively measure both fusion reactions and [3] and (α,p)/(α,n) reactions [9]. Simulations, as detailed in Section 2.2, also indicated that the prescribed anode geometry would contain typical particle ranges for the desired reactions.

The anode was constructed from a printed circuit board in order to have precise spacing between the charge collection segments and easy routing of signal traces. As shown in Fig. 1, the anode is segmented into 18 equal length strips which are then further segmented left–right. Each strip has a width of 1.5 cm with a length of 9 cm. The beam left and right segmentation are 6 cm for the large segments and 3 cm for the small segments. Signals from the first and last strip are not segmented into beam/left right and can be used to veto beam like ions if desired. Signals from strips 1–16 are the active strips, from which the energy loss is measured and the cross section extracted.

The Frisch-Grid is constructed out of a copper frame over which Cu–Be wire is strung. Parameters for the Frisch-Grid wire diameter (0.1 mm) and pitch (1 mm) were calculated using the method described in [12]. The field shaping electrodes and cathode were constructed from 0.79-mm and 3.18-mm aluminum plates, respectively.

The 32 channels from the active strips are fed through the chamber via Mesytec high density shielded cables. Those signals are then sent to two Mesytec MPR16 Charge Sensitive Preamplifiers which are then shaped by Mesytec MSCF16 Shaping Amplifiers. Energy signals from the Cathode, first and last Anode strip, and Frisch-Grid can be read out using standard NIM Modules for amplifying and shaping of the signals. The positive ion signal induced on the cathode was fed through a fast filter amplifier and used as a trigger for data acquisition.

A gas handling system was employed in order to maintain a constant pressure within the detector during operation. The system utilized an Edwards Datametrics Type 1501 A pressure/flow controller and corresponding control valve to maintain a constant pressure. Pressure was monitored throughout operation via a MKS 902B piezo vacuum pressure transducer.

2.3. Simulations

In order to predict and understand the detector response, simulations were performed to calculate the energy losses of the beam and reaction products as they pass through the target gas. Energy loss predictions were calculated via programs such as TRIM, LISE++, or STOPIT [13–15]. These programs allow user input for parameters such as gas pressure and species of target and beam to estimate energy loss, however they are limited in their ability to change these parameters dynamically. Hence, a script was written in Python to define input parameters for the energy loss programs based on a given particle's location in the detector. This script can also be used to inform input parameters for the energy loss of reaction products based off the two-body kinematics of the reaction. By simulating multiple events and randomly sampling where in the detector these reactions occur as well as the angle of the heavy reaction product, we are able to characterize the expected peak energy loss and ranges of reaction products within the detector. Simulated traces for ^{12}C + ^{12}C fusion in ATHENA are shown in Fig. 5

It is important to note that energy loss calculations produced from programs such as TRIM and LISE++ can differ from experiment by as much as 10 percent, and therefore it is important to calibrate the simulations with experimental energy loss measurements. Methods for directly measuring the stopping power of the beam and reaction products are demonstrated in [16].

3. Alpha source test

Before performing experiments with beam in the detector, measurements were made with an alpha source to test detector performance. A mixed alpha source was used consisting of ^{148}Gd and ^{241}Am emitting alphas at 3.18 MeV and 5.49 MeV, respectively. The source was held in place using a 3D printed mount that allowed the placement of the source at the front of the detector pointed towards the back of the detector. The mount also collimated the alpha particles, which are otherwise emitted isotropically from the source. The location and collimation of the source ensured that the alpha particles would travel in roughly the same path as a beam passing through the detector. P10 (10% Methane and 90% Argon) gas was used in the chamber at 150 Torr.

Trace plots show the energy loss of the alpha particles through the detector in Fig. 4. Having a lower energy, the 3.18 MeV shows a shorter range than that of the higher energy 5.49 MeV alpha. Also shown in Fig. 4, is the residual energy of the alpha particles, displaying two distinct energies. The extracted energy resolution was 273 keV for the 3.18 MeV alpha peak, and 310 keV for the 5.49 MeV alpha peak. It should be noted that these resolution values reflect summing multiple anodes together. The resolution for a single anode is much better and on the order of 100 keV.

4. ^{12}C + ^{12}C commissioning measurement

4.1. Measurement

For the commissioning of the detector, the ^{12}C+^{12}C fusion reaction was measured. This reaction was chosen primarily because the cross section has been measured using the MUSIC detector and is well understood in the center of mass region from 40 MeV down to 10 MeV [17]. Another advantage of this reaction is the large difference in energy loss between the beam and evaporation residues, which makes it easier to distinguish between beam-like traces and traces from evaporation residues. Energy resolutions of 2 MeV are more than sufficient for such fusion studies and are easily met by the 100-keV resolution we typically obtain with ATHENA.

A 41 MeV ^{12}C beam was delivered to ATHENA from the FN Tandem accelerator. To reduce the beam rate bombarding the detector, a pair of 1/2000 attenuators were placed in the beamline preceding the detector. The maximum acceptance rate of the detector was determined to be 4000 particles per second as this was the maximum rate the data acquisition could accept without exhibiting significant dead time. Pile-up was found to be insignificant at these rates.

CH_4 gas was used as the target in ATHENA. The beam lost approximately 3 MeV through a 6.25 μm mylar window and 20 MeV through 150 Torr of CH_4 gas. This gave energy loss steps of approximately 1.5 MeV in the c.m. energy frame for each individual strip. This allowed measurements of the total fusion cross section over a c.m. energy from approximately 18 MeV down to 12 MeV.

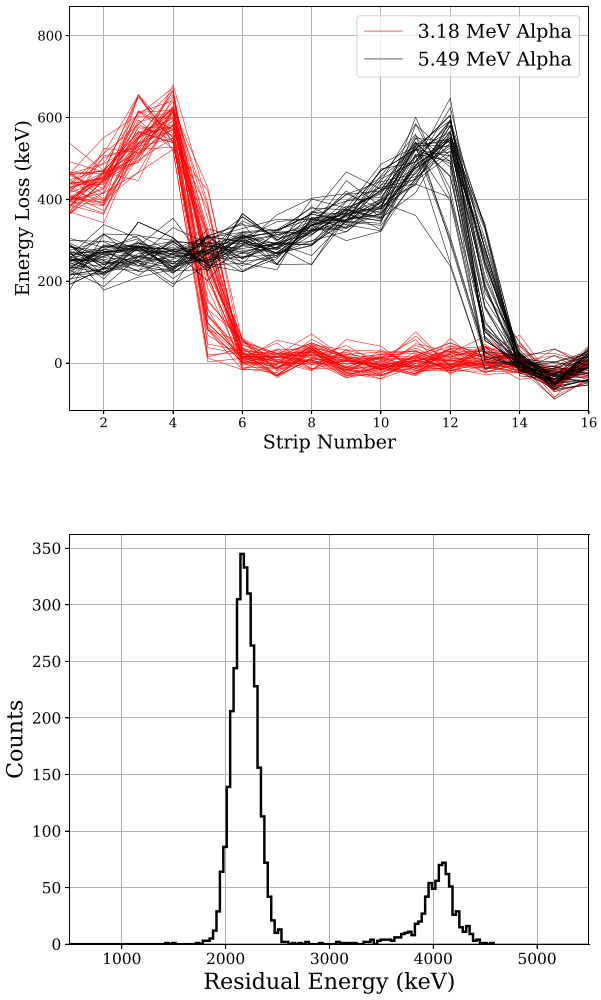

Fig. 4. (top) Traces of the low- and high-energy alpha particles from the mixed alpha source. (bottom) The residual energy of the alpha particles reconstructed from summing the energy losses through ATHENA. The residual energies are lower than the emitted alpha energies due to energy loss in the dead space between the source and the active strips.

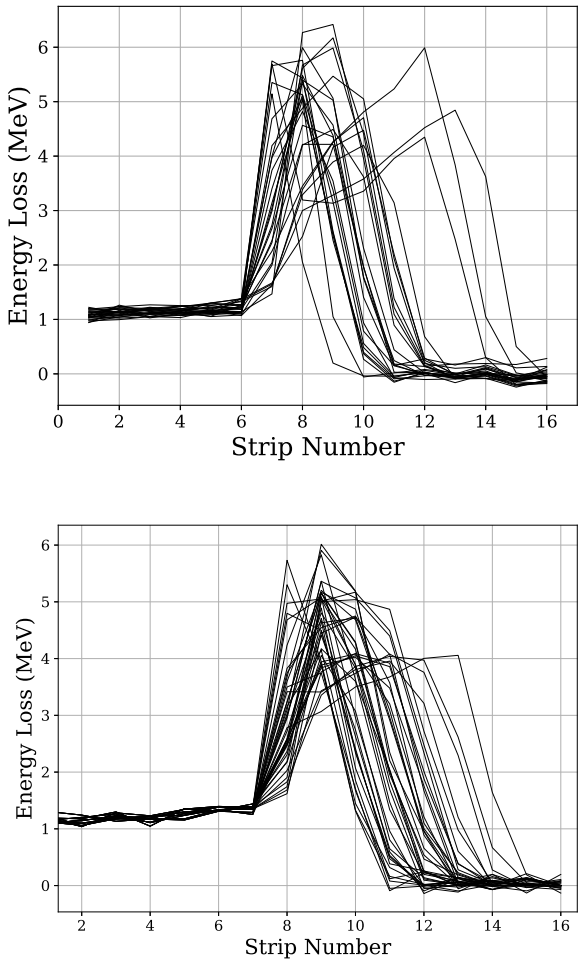

Fig. 5. (top) Selection of evaporation residues produced from strip 7. The characteristic trace of the evaporation residues are shown as a sudden rise in energy followed by decrease back to zero. (bottom) Simulated fusion events for strip 7 using the same beam energy and pressure settings as the above measured events.

4.2. Analysis

In order to identify fusion evaporation residues, an event-by-event analysis was performed. The aim of the process was to filter out events until only evaporation residues are identified. The first step in this process is to normalize the energy of all of the strips to the first strip. This makes the gating process in the subsequent steps in the analysis easier as all beam-like events will occur at the same energies. After normalization, events were gated on beam-like events in the first strip to eliminate reaction events occurring in the window or the dead space before the first strip. This condition will also remove any pile-up events.

Similar to the analysis process followed in [4], a correlated energy loss plot can be helpful for identifying different types of events in each strip. A plot of the correlated single strip energy loss in strip three versus the total energy deposited in the detector for each event is show in Fig. 6. The only condition applied to events shown in this figure is that the events have a beam-like trace in the first strip. Beam-like traces are considered traces that are within a one standard deviation of the mean beam energy.

The most intense feature in this spectrum, labeled beam, corresponds to events that have beam-like traces throughout the detector. There are two features in this spectrum labeled scattering. Extending vertically from the beam are events corresponding to scattering in the target gas. A representative trace of these events is shown in Fig. 7. The other scattering feature, extending diagonally from the beam, are events corresponding to scattering in the Mylar window. The feature label E.R.s extending horizontally from the beam are evaporation residues from reactions occurring after strip 3. These events have a

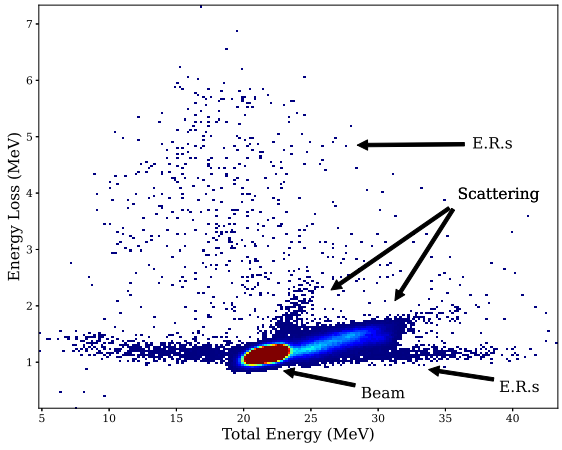

Fig. 6. Correlated energy loss of events in strip three versus total energy loss in detector. Various features of this plot are described in the text.

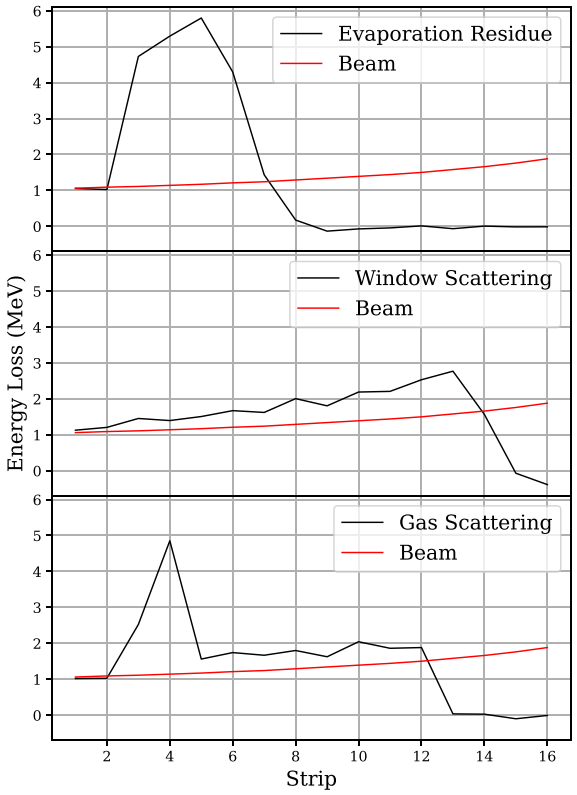

Fig. 7. (top) Trace of evaporation residue from reaction occurring in strip 3. (middle) Trace of window scattering event. (bottom) Trace of gas scattering event.

beam-like energy loss in strip 3, but a total energy differing from that of the beam. Finally events with an energy loss higher than the beam, also labeled E.R.s, represent fusion evaporation residues occurring in, or before to strip 3. A characteristic fusion evaporation residue occurring in strip 3 is shown in Fig. 7.

In order to isolate evaporation residues for reactions in each strip, the following analysis was applied. First, a condition applied is that all preceding strips to the strip being analyzed are gated on beam-like energy loss signals. This ensures that the trajectory of particles before the strip of interest are that of the beam, and eliminates reactions occurring before the reaction strip. For the reaction strip, a condition is placed that events have an energy loss higher than that of the beam by one standard deviation. This will eliminate trajectories that are beam-like in following strips and should leave only scattering, proton-capture, and fusion events in the analyzed strip.

To reject some portion of scattering events and proton capture events, a condition is placed that the event has an energy lower than that of the beam by the time it reaches the last strip. This will eliminate these events on the basis that they have longer ranges than that of the evaporation residues. This condition, however, is not applied for reactions in the last 6 strips. This is due to the range of the particles being outside the active region. This process is repeated for each strip where the range of evaporation residues are well contained within the detector (i.e., strips 2 through 12). Scattering events can also be further eliminated by analyzing the shape of their trace. As demonstrated in Fig. 7, gas scattering events have a characteristic shape where a sudden change in energy loss occurs followed by a relatively level energy loss trace. A trace plot showing a selection of evaporation residues from reactions in the 7th strip is shown in Fig. 5.

Once the reaction events were identified, the reaction cross section was calculated from

$$\sigma_{tot} = \frac{N_{ERs}}{N_{Beam} * A} \quad (1)$$

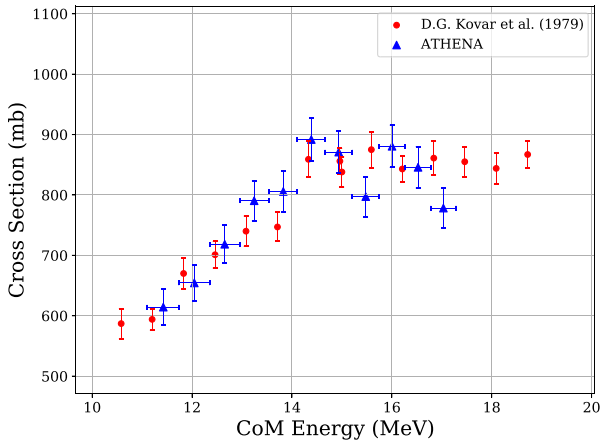

Fig. 8. $^{12}C + {}^{12}C$ Total Fusion Cross Section extracted from ATHENA.

where N_{ERs} is the total number of fusion events, N_{Beam} is the total number of beam events and A is the target areal density as given by the gas pressure and ambient temperature in the chamber. The total fusion cross section for this $^{12}C + {}^{12}C$ fusion experiment is shown in Fig. 8. The error in cross section is given by statistical uncertainty, whereas the uncertainty in energy is determined by the width of the strip since there is an ambiguity of where in the strip the reaction occurred. To assign the central energy point for each strip some consideration is needed. In each strip the beam loses more energy in the second half of the strip than the first, thus the cross section should be weighted towards higher energy. In order to account for this, the central point is weighted by previous cross section measurements made by Kovar et al. [18]. Each strip is divided into sections and then the energy is weighted by the interpolated cross section value for each division. As shown in Fig. 8, the results agree favorably with previous measurements.

5. Summary

A new active target detector, ATHENA, has been built for measuring total cross sections of astrophysical interest. With a segmented anode, total energy and angle integrated cross sections can be measured with high efficiency without having to change the energy of the incoming beam. Due to ATHENA's limit in incoming beam rate, it is well suited to measure reactions with low intensity radioactive beams provided by TwinSol.

The detector was commissioned by measuring the $^{12}C + {}^{12}C$ total fusion cross section from an energy range of approximately 18 MeV down to 12 MeV. This first measurement allowed for easy identification of the evaporation residues due to their large change in energy loss relative to that of the beam. An extensive event filtering process allows for the accurate identification of evaporation residues.

One drawback of the current detector setup is the inability to get absolute measurements of beam energy through the gas. While the detector gives relative energy loss, a direct measurement of the energy loss through the detector will give more precise determinations of the reaction cross section energy without having to rely on energy loss predictions. This can be done by attaching a Si detector to a linear drive and having it measure the beam as it passes through each strip similar to Ref. [4]. This process is being implemented in ATHENA for future measurements.

Declaration of competing interest

The authors declare the following financial interests/personal relationships which may be considered as potential competing interests: Drew Blankstein reports financial support was provided by National Science Foundation.

Data availability

Data will be made available on request.

Acknowledgments

The authors would like to acknowledge useful conversations with R. deSouza and B. DiGiovine. This work was supported by the National Science Foundation, USA under grant No. PHY-2011890 and by the University of Notre Dame, USA.

References

[1] D. Bazin, T. Ahn, Y. Ayyad, S. Beceiro-Novo, A. Macchiavelli, W. Mittig, J. Randhawa, Low energy nuclear physics with active targets and time projection chambers, Prog. Part. Nucl. Phys. 114 (2020) 103790, http://dx.doi.org/10.1016/j.ppnp.2020.103790, URL https://www.sciencedirect.com/science/article/pii/S0146641020300375.

[2] S. Beceiro-Novo, T. Ahn, D. Bazin, W. Mittig, Active targets for the study of nuclei far from stability, Prog. Part. Nucl. Phys. 84 (2015) 124–165, http://dx.doi.org/10.1016/j.ppnp.2015.06.003, URL https://www.sciencedirect.com/science/article/pii/S0146641015000459.

[3] P. Carnelli, S. Almaraz-Calderon, K. Rehm, M. Albers, M. Alcorta, P. Bertone, B. Digiovine, H. Esbensen, J.F. Niello, D. Henderson, C. Jiang, J. Lai, S. Marley, O. Nusair, T. Palchan-Hazan, R. Pardo, M. Paul, C. Ugalde, Multi-sampling ionization chamber (MUSIC) for measurements of fusion reactions with radioactive beams, Nucl. Instrum. Methods Phys. Res. A 799 (2015) 197–202, http://dx.doi.org/10.1016/j.nima.2015.07.030, URL http://www.sciencedirect.com/science/article/pii/S0168900215008591.

[4] J. Johnstone, R. Kumar, S. Hudan, V. Singh, R. deSouza, J. Allen, D. Bardayan, D. Blankstein, C. Boomershine, S. Carmichael, A. Clark, S. Coil, S. Henderson, P. O'Malley, Music@Indiana: An effective tool for accurate measurement of fusion with low-intensity radioactive beams, Nucl. Instrum. Methods Phys. Res. A 1014 (2021) 165697, http://dx.doi.org/10.1016/j.nima.2021.165697, URL https://www.sciencedirect.com/science/article/pii/S0168900221006823.

[5] B. Asher, S. Almaraz-Calderon, L. Baby, N. Gerken, E. Lopez-Saavedra, A. Morelock, J. Perello, The encore active target detector: A multi-sampling ionization chamber, Nucl. Instrum. Methods Phys. Res. A 1014 (2021) 165724, http://dx.doi.org/10.1016/j.nima.2021.165724, URL https://www.sciencedirect.com/science/article/pii/S0168900221007099.

[6] W. Christie, J. Romero, F. Brady, C. Tull, C. Castaneda, E. Barasch, M. Webb, J. Drummond, H. Crawford, I. Flores, D. Greiner, P. Lindstrom, H. Sann, J. Young, A multiple sampling ionization chamber (MUSIC) for measuring the charge of relativistic heavy ions, Nucl. Instrum. Methods Phys. Res. A 255 (3) (1987) 466–476, http://dx.doi.org/10.1016/0168-9002(87)91213-7, URL https://www.sciencedirect.com/science/article/pii/0168900287912137.

[7] K. Kimura, Y. Akiba, Y. Miake, S. Nagamiya, A multiple sampling proportional counter for particle identification of relativistic heavy ions, Nucl. Instrum. Methods Phys. Res. A 297 (1) (1990) 190–198, http://dx.doi.org/10.1016/0168-9002(90)91366-J, URL https://www.sciencedirect.com/science/article/pii/016890029091366J.

[8] R.N. Boyd, I. Tanihata, N. Inabe, T. Kubo, T. Nakagawa, T. Suzuki, M. Yonokura, X.X. Bai, K. Kimura, S. Kubono, S. Shimoura, H.S. Xu, D. Hirata, Measurement of the ^{8}Li(α,n)^{11}b reaction cross section at energies of astrophysical interest, Phys. Rev. Lett. 68 (1992) 1283–1286, http://dx.doi.org/10.1103/PhysRevLett.68.1283, URL https://link.aps.org/doi/10.1103/PhysRevLett.68.1283.

[9] M. Avila, K. Rehm, S. Almaraz-Calderon, A. Ayangeakaa, C. Dickerson, C. Hoffman, C. Jiang, B. Kay, J. Lai, O. Nusair, R. Pardo, D. Santiago-Gonzalez, R. Talwar, C. Ugalde, Study of (α ,p) and (α ,n) reactions with a multi-sampling ionization chamber, Nucl. Instrum. Methods Phys. Res. A 859 (2017) 63–68, http://dx.doi.org/10.1016/j.nima.2017.03.060, URL https://www.sciencedirect.com/science/article/pii/S0168900217304187.

[10] M. Lee, F. Becchetti, T. O'Donnell, D. Roberts, J. Zimmerman, V. Guimarães, J. Kolata, D. Peterson, P. Santi, P. DeYoung, G. Peaslee, J. Hinnefeld, Study of nuclear reactions with intense, high-purity, low-energy radioactive ion beams using a versatile multi-configuration dual superconducting-solenoid system, Nucl. Instrum. Methods Phys. Res. A 422 (1) (1999) 536–540, http://dx.doi.org/10.1016/S0168-9002(98)01081-X, URL https://www.sciencedirect.com/science/article/pii/S016890029801081X.

[11] J.F. Ziegler, Stopping of energetic light ions in elemental matter, J. Appl. Phys. 85 (3) (1999) 1249–1272, http://dx.doi.org/10.1063/1.369844.

[12] O. Bunemann, T.E. Cranshaw, J.A. Harvey, Design of grid ionization chambers, Can. J. Res. 27a (5) (1949) 191–206.

[13] J.F. Ziegler, M. Ziegler, J. Biersack, SRIM – the stopping and range of ions in matter (2010), Nucl. Instrum. Methods Phys. Res. B 268 (11) (2010) 1818–1823, http://dx.doi.org/10.1016/j.nimb.2010.02.091, URL http://www.sciencedirect.com/science/article/pii/S0168583X10001862, 19th International Conference on Ion Beam Analysis.

[14] O. Tarasov, D. Bazin, LISE++: Exotic beam production with fragment separators and their design, Nucl. Instrum. Methods Phys. Res. B 376 (2016) 185–187, http://dx.doi.org/10.1016/j.nimb.2016.03.021, URL https://www.sciencedirect.com/science/article/pii/S0168583X1600224X. Proceedings of the XVIIth International Conference on Electromagnetic Isotope Separators and Related Topics (EMIS2015), Grand Rapids, MI, U.S.A., 11-15 May 2015.

[15] K. Braune, R. Novotny, D. Pelte, D. Husar, D. Schwalm, Proceedings of the Spring Meeting of the German Physical Society, Vol. 4, German Physical Society, 1978.

[16] J. Johnstone, R. Kumar, S. Hudan, R. deSouza, J. Allen, D. Bardayan, D. Blankstein, C. Boomershine, S. Carmichael, A. Clark, S. Coil, S. Henderson, P. O'Malley, Improving the characterization of fusion in a MuSIC detector by spatial localization, Nucl. Instrum. Methods Phys. Res. A 1025 (2022) 166212, http://dx.doi.org/10.1016/j.nima.2021.166212, URL https://www.sciencedirect.com/science/article/pii/S0168900221010706.

[17] S. Almaraz-Calderon, P. F. F. Carnelli, K. E. Rehm, M. Albers, M. Alcorta, P. F. Bertone, B. Digiovine, H. Esbensen, J. Niello, D. Henderson, C. L. Jiang, J. Lai, S. T. Marley, O. Nusair, T. Palchan, R. Pardo, M. Paul, C. Ugalde, C+C fusion cross sections measurements for nuclear astrophysics, EPJ Web Conf. 96 (2015) 01001, http://dx.doi.org/10.1051/epjconf/20159601001.

[18] D.G. Kovar, D.F. Geesaman, T.H. Braid, Y. Eisen, W. Henning, T.R. Ophel, M. Paul, K.E. Rehm, S.J. Sanders, P. Sperr, J.P. Schiffer, S.L. Tabor, S. Vigdor, B. Zeidman, F.W. Prosser, Systematics of carbon- and oxygen-induced fusion on nuclei with $12 \leq A \leq 19$, Phys. Rev. C 20 (1979) 1305–1331, http://dx.doi.org/10.1103/PhysRevC.20.1305, URL https://link.aps.org/doi/10.1103/PhysRevC.20.1305.